Targeted Delivery of Amantadine-loaded Methacrylate Nanosphere-ligands for the Potential Treatment of Amyotrophic Lateral Sclerosis

Zamanzima Mazibuko[1], Sunaina Indermun[1], Mershen Govender[1], Pradeep Kumar[1], Lisa C. du Toit[1], Yahya E. Choonara[1], Girish Modi[2], Dinesh Naidoo[3] and Viness Pillay[1*]

[1] Wits Advanced Drug Delivery Platform Research Unit, Department of Pharmacy and Pharmacology, School of Therapeutic Sciences, Faculty of Health Sciences, University of the Witwatersrand, Johannesburg, 7 York Road, Parktown, 2193, South Africa. [2] Department of Neurology, Division of Neurosciences, Faculty of Health Sciences, University of the Witwatersrand, Johannesburg, 7 York Road, Parktown, 2193, South Africa. [3] Department of Neurosurgery, Division of Neurosciences, Faculty of Health Sciences, University of the Witwatersrand, Johannesburg, 7 York Road, Parktown, 2193, South Africa.

Received, September 29, 2017; Accepted, February 26, 2018; Published, March 1, 2018.

ABSTRACT - Purpose. This study aimed to develop and analyse poly(DL-lactic acid)-methacrylic acid nanospheres bound to the chelating ligand diethylenetriaminepentaacetic acid (DTPA) for the targeted delivery of amantadine in Amyotrophic Lateral Sclerosis (ALS). **Methods.** The nanospheres were prepared by a double emulsion solvent evaporation technique statistically optimized employing a 3-Factor Box-Behnken experimental design. Analysis of the particle size, zeta potential, polydispersity (Pdl), morphology, drug entrapment and drug release kinetics were carried out. **Results.** The prepared nanospheres were determined to have particle sizes ranging from 68.31 to 113.6 nm (Pdl $\leq$ 0.5). An initial burst release (50% of amantadine released in 24 hr) was also obtained, followed by a prolonged release phase of amantadine over 72 hr. Successful conjugation of the chelating ligand onto the surface of the optimised nanospheres was thereafter achieved and confirmed by TEM. The synthesized modified nanospheres were spherical in shape, 105.6 nm in size, with a PdI of 0.24 and zeta potential of -28.0 mV. Conjugation efficiency was determined to be 74%. *In vitro* and *ex vivo* cell study results confirmed the intracellular uptake of the modified nanospheres by the NSC-34 cell line and the non-cytotoxicity of the synthesized nanospheres. **Conclusions.** Biocompatible amantadine-loaded nanospheres were successfully designed, characterized and optimized employing the randomized Box-Behnken statistical design. Delivery of amantadine over 72 hrs was achieved, with the nanospheres being of a size capable of internalization by the NSC- 34 cells.

INTRODUCTION

Motor neuron disease (MND) refers to a group of progressive neurodegenerative disorders which are distinguished by the deterioration of upper motor neurons and/or lower motor neurons (1). The disorder known as Amyotrophic Lateral Sclerosis (ALS) results in the degeneration of both upper and lower motor neurons and has the most cases reported. The frequency of this disease is approximately 2 in 100 000 with an average age of onset of 58 years (2). The expected survival from the initiation of the symptoms is 3 years. In approximately 90% of the cases, the disease occurs sporadically (Sporadic ALS) whereas the remaining 10% is inherited or familial (Familial ALS) (3). Many mechanisms appear to contribute to the neurodegenerative progression and comprise of protein aggregation, glutamatergic toxicity, mitochondrial dysfunction, oxidative stress, neuroinflammation, cytoskeletal derangements, growth factor dysregulation, apoptosis as well as high expression of the copper, zinc-superoxide dismutase (Cu, Zn-SOD) enzyme (3, 4). A variety of anomalous oxidative reactions catalysed by this mutant enzyme has been proposed to contribute to the neurodegeneration whereby the conformation of the mutant enzyme is more open, allowing substrates other than superoxide to penetrate the active site and react with the copper and zinc ions enclosed within (5, 6).

Although chelating therapy holds great potential in managing neurodegenerative disorders, factors such as bypassing the blood-brain barrier and toxic side effects remain

Corresponding Author: Professor Viness Pillay, 8M09 Department of Pharmacy and Pharmacology, Wits Medical School, 7 York Road, Parktown 2193, Johannesburg, South Africa. Email: viness.pillay@wits.ac.za;

problematic (7). This translates to difficulties in treating disorders in the central nervous system (CNS) because of low bioavailability of drugs resulting from both biopharmaceutical and physiological factors. Nanoparticulate delivery systems are however able to overcome these barriers by avoiding systemic degradation and penetrating tight junctions to deliver therapeutic agents to their target sites. In addition, they offer drug release for desired time periods, thereby improving therapeutic efficacy and reducing drug toxicity (8, 9, 10). Conjugation of these nanoparticles furthermore can assure site-specific aggregation of drug at the target site, ensuring maximum therapeutic effects in addition to a decreased dose and decreased side effects. Amantadine, the model drug for this study, has been used extensively for its anti-parkinsonian effects in neurodegenerative disorders and particularly amyotrophic lateral sclerosis. This is achieved through its induction of dopamine synthesis and release as well as its blockage of the reuptake of dopamine, increasing availability for dopaminergic receptor activation.

The aim of this study was therefore to design, develop and evaluate a nanoparticulate-thermoresponsive gel delivery system able to bypass the blood-brain barrier and enhance cellular uptake and biodistribution of therapeutic agents without presenting cytotoxicity. Hydrogels have been extensively utilized as drug delivery systems for sustained delivery of drugs *in vivo* thereby allowing for large dose to be administered without the risk of dose-dependent side effects (11). The use of the thermoresponsive hydrogel further allows for ease of production and administration where the hydrogel transitions from a solution state at ambient temperature to a gel state at physiological temperature (12). The amantadine-loaded nanospheres used within the thermoresponsive were prepared and optimized using a Box-Behnken statistical design and thereafter bound with the chelating ligand diethylenetriaminepentaacetic acid (DTPA), a polyaminocarboxylic acid which can remove several ions including copper and zinc (13). Extensive *in vitro* characterization has been carried out on the amantadine nanospheres, the conjugated nanosphere-ligands as well as the conjugate nanospheres in the thermoresponsive hydrogel. *Ex vivo* cellular uptake and toxicity studies have also been undertaken using on the motor neuron NSC-34 cell line, a hybrid cell-line fusing motor neuron-enriched embryonic mouse spinal cord cells with mouse neuroblastoma.

MATERIALS AND METHODS

MATERIALS

Polymethacrylate (PMA; Eudragit L100) was purchased from Degussa, Rohm GmbH, Pharma Polymers (Germany). Poly(D,L-lactide) (PLA), Diethylenetriaminepentaacetic acid (DTPA), N-Hydroxysuccinimide (NHS), N,N'-Dicyclohexylcarbodiimide (DCC), amantadine hydrochloride, N-vinylcaprolactam (VCL), ε-Caprolactone, 2,2'-Azobis (2 methyl-propionitrile) (AIBN), Dulbelccos Minimum Essential Medium (DMEM), Trypan Blue Solution (0.4%), MTT (3-(4, 5 – Dimethylthiazol – 2 – y l) – 2 , 5 diphenyltetrazolium bromide), Fluorescein isothiocyanate (FITC) and dimethyl sulphoxide (DMSO) were all purchased from Sigma-Aldrich (St Louis, MO, USA). NSC-34 cells were obtained from Cedarlane Laboratories (Burlington, Ontario, Canada). Fetal bovine serum (FBS) and Penicillin-Streptomycin (Pen-Strep) were purchased from Highveld Biological (Modderfontein, Gauteng, South Africa). All other chemicals were of analytical grade and were used as purchased.

Preparation and optimization of the amantadine-loaded nanospheres

Amantadine-loaded nanospheres were prepared by a double-emulsion solvent evaporation technique utilizing ultrasonication. Briefly, the internal aqueous phase was prepared by dissolving 100 mg of amantadine in 1 mL of deionized water. The organic phase was prepared by dissolving both polymers, PLA and PMA, in a solvent mixture of dichloromethane and isopropyl alcohol in a 1:1 ratio. The internal aqueous phase and organic phase were thereafter ultrasonicated for 3 min at room temperature to form a primary emulsion. The external phase was prepared by dissolving Span 80 in phosphate buffer saline (PBS, pH 7.4) to form a 0.025% $^{v}/_{v}$ solution. The primary emulsion was then added drop-wise to the external aqueous phase followed by ultrasonication to form nanospheres. The formed nano-emulsion was thereafter centrifuged at 15000 rpm for 20 min at room temperature to recover the nanospheres. The nanospheres were then washed twice with distilled water and thereafter lyophilized (Lanconco, Kansas City, MS, USA) for 24 hr.

Experimental design and constraint optimization of the amantadine-loaded nanospheres

A three-factor, three-level Box-Behnken statistical

design (MINITAB® V14, State College, Pennsylvania, USA) was used to optimize the amantadine-loaded PLA-PMA nanospheres. Statistical optimization was employed to ascertain the ideal combination of ultrasonication time, solvent volume and amount of polymer (PMA) used capable of attaining the desirable particle size, zeta potential, drug entrapment efficiency and mean dissolution time (MDT). Table 1 summarizes the fifteen experimental runs studied, their factor combinations and the translation of the coded levels to the experimental units employed during the study. The results obtained subsequently produced independent parameter values for the optimized formulation as well as the expected responses.

Determination of particle size distribution, zeta potential and polydispersity index

The size distribution, zeta potential and polydispersity index (PDI) of the nanospheres were assessed using a Zetasizer Nano ZS system (Malvern Instruments Ltd, Malvern, Worcestershire, UK) at 25 °C. Briefly, aliquots of 0.8 mL of the nanosphere emulsion were placed into the appropriate cuvette and the software configured with the specific parameters of refractive index and absorption coefficient of the nanomaterials and solvent viscosity.

Determination of the amantadine-loading capacity of the prepared nanospheres

The amantadine-loaded nanospheres (10 mg) were accurately weighed and were resuspended in 10ml of PBS (pH 7.4; 37 °C) for a period of 7 days. The samples were then centrifuged at 2500 rpm for 30 min followed by a reaction of the supernatant with potassium permanganate ($KMNO_4$) for 15 min at room temperature (14). The absorbances of the resulting solutions were measured at 525 nm (ε=0.1023) by UV spectrophotometry (Lambda 25, UV/VIS Spectrometer, PerkinElmer®, Waltham, MA, USA) against a reagent blank and computed from a standard linear curve of the drug in PBS to determine amantadine content. The theoretical amount of amantadine was considered as the proportional amount of amantadine in 10 mg of nanospheres referenced to the loading dose.

***In vitro* drug release studies**

In vitro drug release analyses were carried out for 72 hrs using an orbital shaking incubator set at 25 rpm. The amantadine-loaded nanospheres, housed in dialysis tubing, were immersed in 50 mL PBS (pH 7.4, 37 °C) in glass jars. At predetermined time intervals, 2 mL samples of the release media were removed and replaced with fresh buffer of the same volume to maintain sink conditions. The samples were centrifuged and the supernatant reacted with potassium permanganate and subsequently analyzed by UV spectroscopy (14). Mean dissolution time (MDT) was used to analyze the ability of the nanospheres to control amantadine release.

Table 1. 3-factor Box-Behnken experimental design for PLA-PMA nanosphere formulation.

Formulation	PMA (mg)	Ultrasonication time (min)	Solvent volume (mL)
1	210	20	15
2	160	20	20
3	210	30	20
4	210	20	15
5	210	20	15
6	260	20	10
7	260	10	15
8	260	20	20
9	160	10	15
10	210	30	10
11	160	20	10
12	210	10	10
13	210	10	20
14	260	30	15
15	160	30	15

Turbidity assessment of the optimized nanosphere emulsion

The stability of the nanosphere emulsion was assessed by employing a Turbiscan Lab® Stability Analyzer (Turbiscan Lab™, Formulaction SA, L'Union, France). Measurements were performed at 25°C and the Turbiscan Lab® was configured to perform scans for 5 min, over a 55 mm cell length, from bottom to top acquiring transmission and backscattering data every 40 μm. Deviation in particle volume fraction on particle migration and the mean particle diameter attributable to coalescence resulted in variation in the magnitude of transmitted and back-scattered light. The measured amount of transmitted and backscattered light was then interpreted and used to describe the dispersion state (stability) of the emulsion.

Analysis of the surface morphology of the nanospheres

Transmission electron microscopy (TEM, JEOL 1200 EX, Japan) was performed on the nanosphere emulsion following initial ultrasonication at a relative amplitude of 80 for 1 min (20 kHz sonicator, VibraCell, Sonics and Materials, Inc., Danbury, CT, USA). One drop of the emulsion was placed onto the copper TEM sample grid and allowed to dry (~20 min) before being placed into the TEM airlock/ specimen stage. Images were acquired at 10 000x magnification.

Preparation of the nanosphere-DTPA ligand

The amantadine-loaded nanospheres were resuspended in 20 mL of PBS (pH 7.4). Separately, DCC was dissolved in 5 mL of dichloromethane. The two solutions were mixed together under magnetic stirring for 1 hr. The dichloromethane was thereafter removed by rotary evaporation (Rotavapor® RII, Büchi Labortechnik AG, Switzerland) at 65 °C for 1 hr. Simultaneously, NHS and DTPA were dissolved in PBS (pH 7.4) under magnetic stirring for 3 hr. Resulting in the N-hydroxysuccinimide active ester of DTPA (15, 16). The two solutions were then combined and stirred for a further 4 hr. The final solution was incubated at 4 °C and thereafter centrifuged and washed twice with deionized water to remove any unbound DTPA.

Assessment of the conjugation efficiency of the nanosphere-DTPA ligand

The evaluation of the conjugation efficiency of DTPA on the surface of the nanospheres was conducted employing UV. The NHS-DTPA ester and hence the conjugated nanospheres in solution was read at a maximum wavelength of λ_{260} against a blank sample of unmodified nanospheres samples in a 10 mM ammonium acetate buffer (pH 7.4) (17).

Preparation and *in vitro* analysis of the amantadine-loaded-DTPA bound nanospheres suspended in a thermoresponsive hydrogel

For the thermoresponsive hydrogel, adapted from Wu and co-workers (18), 2.5 g of VCL and 0.2 mL of ε-Caprolactone were dissolved in 20 mL of isopropanol. The reaction mixture was thereafter flushed with nitrogen for 30 min. The solution was then dissolved in distilled water and the isopropyl alcohol removed by rotary evaporation. AIBN (0.2 mL) was added to the remaining solution followed by overnight incubation in a sealed vessel at 60 °C to form a sol. *In vitro* drug release studies on nanosphere drug delivery system were carried out for 72 hrs as detailed previously. Structural validation of the conjugated nanosphere-hydrogel system using Fourier Transform Infrared Spectroscopy (FTIR) can be found in the supplementary data. Wu and co-workers (18) have extensively investigated the thermoresponsive properties of VCL -ε-Caprolactone. Thus to investigate and adapt the co-polymeric hydrogel to this delivery system, the nanosphere release temperature was investigated at the physiological temperature of 37° C. the intended temperature of application.

Determination of the viscoelastic region of the thermoresponsive hydrogel

To determine the viscoelastic region of the hydrogel formulation, the sample was placed on the lower plate of a Haake Modular Advanced Rheometer System (ThermoFisher Scientific, Germany) where the yield stress of the formulation was first determined, as this is the point at which a minimum critical shear stress is exceeded and therefore the point at which a viscoelastic substance begins to flow. Stress sweeps at 0.01 Hz, 1 Hz and 10 Hz were then conducted ensuring that the minimum strain applied was less than the yield stress value obtained. The stress sweep plots were then analyzed and the plateau or linear viscoelastic region where both G' (storage modulus) and G'' (loss modulus) were independent of the stress amplitude, was used as the viscoelastic region. The first point of deviation from the plateau and the frequency at which it occurred was used for subsequent temperature ramping tests. The yield stress was also thus determined.

Establishing the gelation temperature of the thermoresponsive hydrogel

Rheology analysis of the prepared thermoresponsive hydrogel was undertaken using the rheometer system. In order to determine the lower critical solution temperature (LCST) and hence the gelation temperature of the hydrogel formulation, the temperature of the sample was ramped from 10-40˚C at a rate of 0.25 ˚C/min while applying predetermined stress. The gelation temperature was determined as the temperature at which the cross-over of G' and G" occurred i.e., the point at which the formulation was no longer acting as a liquid (G") but the solid phase (G') was dominating.

Surface morphology of the thermoresponsive hydrogel

To visualize the surface morphology of the prepared thermoresponsive hydrogel, a lyophilized sample of the hydrogel was mounted on a specimen stub and gold coated using a SPI-ModuleTM sputter coater (SPI Supplies, STRUCTURE PROBE INC, West Chester, Pennsylvania, USA) and then observed at various magnifications under a scanning electron microscope (SEM) (PHENOMTM Desktop SEM, FEI Company, Oregon, USA) operated at 10KV in the electron imaging mode.

NSC-34 cell culture studies

The NSC-34 cell line was grown using DMEM supplemented with 10 % FBS and 0.25 % Pen-Strep incubated in a humidified 37 °C environment controlled at 5% CO_2. At 80 % confluence, the cells were harvested using trypsin/EDTA and were sub-cultured into 75 cm^2 flasks, 12-well plates on circular glass cover-slides for internalization studies and 96-well plates for the toxicity assays. When the cells had detached, 3 mL of fresh media was added, and the entire volume was centrifuged at 1000 rpm for 3 min. The supernatant was then discarded and the cell pellet resuspended in 8 mL of fresh media and placed into two flasks. The cells were then frozen in a mixture of 60 % growth medium and 30 % FBS supplemented with 10 % sterile DMSO at -80 °C in vials overnight. The vials were then transferred and stored in liquid nitrogen.

Cytotoxicity assay

To determine the cytotoxic effect of DTPA, amantadine, the polymers and the nano-enabled delivery system on the NSC-34 cell line; MTT (3-(4,5-dimethyl-2-thiazolyl)-2,5-diphenyl-2H-tetrazolium bromide) colorimetric assay was applied (n=3). Briefly, asynchronously growing cells were transferred into 96 well culture plates and incubated for 24 hr. The culture medium was replaced with fresh medium containing different concentrations of DTPA and incubated for 24, 48 and 72 hr. The MTT assay was subsequently performed and the cell viability calculated. The absorbances were read off a BioTek Power WaveXS Universal Microplate Spectrophotometer (BioTek Instruments, Inc., USA) equipped with Genesis 5.1 data analysis software. Statistical analysis of the cytotoxicity data was undertaken utilizing Microsoft® Excel software with single-factor analysis of variance (ANOVA) protocols. A P value < 0.05 was considered significant.

Fluorescein-labeling of the conjugated nanospheres

Labelling of the nanospheres was achieved by incubating the conjugated nanospheres under light-protected conditions in Fluorescein Isothiocyanate at a concentration of 2µg/mL for a period of 30 min at 37 °C on a magnetic stirrer. After incubation the nanosphere suspension was centrifuged at 280 x g for 15 min and thereafter were washed 3 times to remove any residual Fluorescein Isothiocyanate.

High speed fluorescence microscopy for live imaging nanosphere uptake by NSC-34 cells

A high-speed fibre-optic fluorescence microscope (Cellvizio® LAB, coupled with Microprobes and ImageCell™ Software; Visualsonics and Mauna Kea Technologies, USA) was utilised for *ex vivo* cellular imaging to determine nanosphere uptake by the NSC-34 cells. Fluorescein-conjugated nanospheres were prepared with each nanosphere suspension (0.5 mL) placed in a graduated sterile centrifuge tube. NSC-34 cell culture (1 mL) was then introduced into each tube followed by centrifugation of the cell cultures at 280 x g in a high-speed table microcentrifuge (Model TG16-WS, Shanghai Ronbio Scientific Co., Ltd., China) with extraction of the supernatant. Thereafter, the cells were re-suspended in PBS (pH 7.4).

RESULTS

Response optimization of the Amantadine-loaded nanospheres

Response optimization (MINITAB®, V15, Minitab, USA) was used to obtain the preferred levels of the selected formulatory components. An optimal formulation was developed following simultaneous constrained optimization of the size

of the nanospheres, zeta potential, amantadine entrapment and mean dissolution time (Table 2). The optimized levels of the independent variables and their predicted responses were then determined. The optimized levels of the independent variables, the goal for the response, the predicted response, y, at the current factor settings, as well as the individual and composite desirability scores are shown in Figure 1a. Figure 1b represents the amantadine release profile of the optimized nanosphere formulation.

Table 2. Response data obtained for the 3-factor Box-Behnken experimental design PLA-MA nanosphere formulations.

Formulation	Size (nm)	Zeta Potential (mV)	Drug Entrapment (%)	MDT (hr)
F1	81.94	-24.7	35.84	21.07
F2	104.4	-21.1	19.43	21.34
F3	81.98	-26.4	33.31	20.12
F4	69.08	-23.2	34.89	21.91
F5	88.22	-27	35.48	19.33
F6	99.99	-25.9	39.75	14.07
F7	75.8	-25.9	39.29	22.5
F8	78.4	-22	38.62	22.47
F9	73.78	-27.1	19.45	12.71
F10	101.2	-14.3	34.08	20.4
F11	68.31	-26.5	19.56	19.54
F12	76.32	-22.8	35.53	15.57
F13	138.1	-23.7	32.97	21.79
F14	112.8	-27.9	38.13	18.1
F15	113.6	-29.2	19.48	21.94

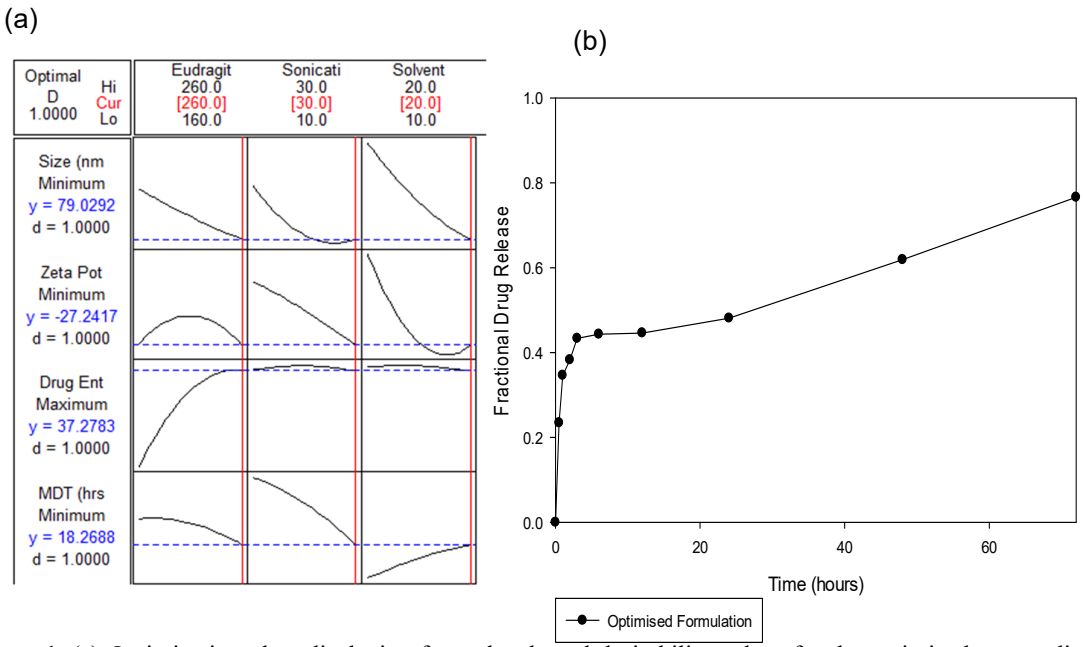

Figure 1. (a) Optimization plots displaying factor levels and desirability values for the optimized amantadine-loaded nanospheres and (b) the drug release profile of the optimized nanosphere formulation (SD ≤0.206 in all cases).

Nanosphere emulsion stability

The delta back scattering profile of the optimized nanosphere emulsion depicted in Figure 2a indicates that the nanosphere emulsion was largely stable. The middle and the bottom of the profile remained consistent indicating that the emulsion was stable over the test duration and no flocculation or coalescence occurred to the nanosphere emulsion during the experiment. There was, however, a small amount of local destabilization which can be seen by the slight wavering in the delta backscattering signal at the top end of the glass cell. Figure 2b indicates that between 32.4-48.1 mm backscattering remained consistent and further confirms that the nanosphere emulsion was stable.

Morphological Characterization of the Modified Nanospheres

TEM micrographs of modified DTPA-bound nanospheres are shown in Figure 3. TEM images revealed spherical and uniform unmodified nanospheres and modified nanospheres. In addition, the images show that the unmodified nanospheres and modified nanospheres synthesized were of a nano-size range. DTPA conjugation is reflected by an aggregation of DTPA-bound nanospheres on the TEM imaging (Figure 3b).

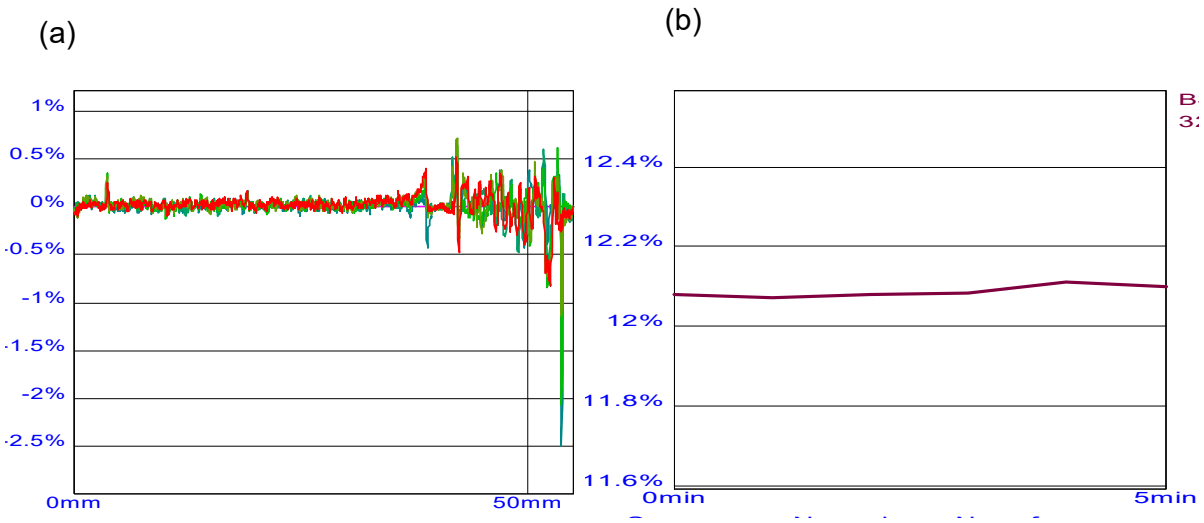

Figure 2. (a) Delta backscattering for the optimized amantadine-loaded nanospheres and (b) Backscattering presented on the cell: 32.4-48.1mm.

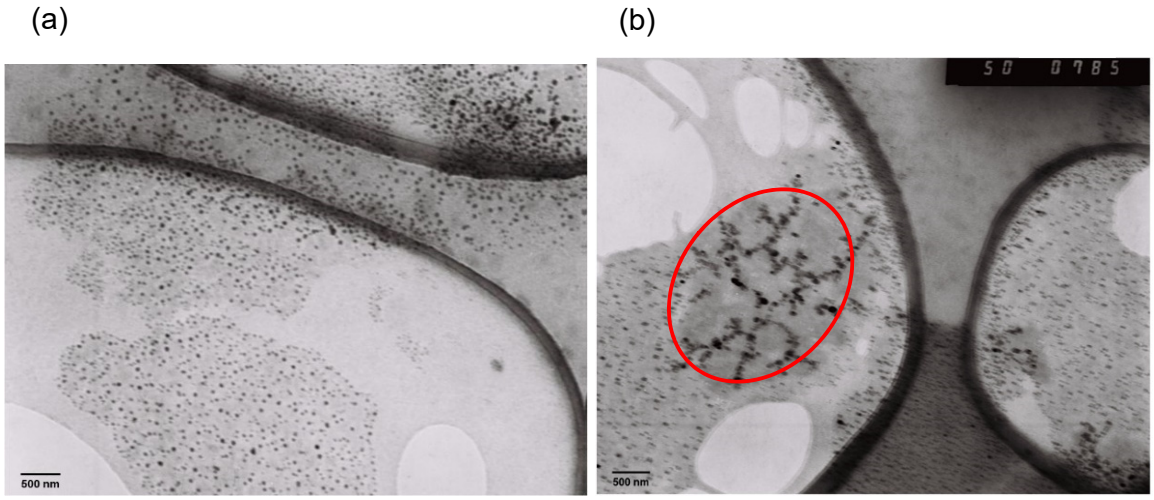

Figure 3. TEM images of a) the unmodified optimized nanospheres and b) the DTPA-bound nanospheres captured at 10,000 x.

Conjugation Efficiency of DTPA on the Surface of the Nanospheres

The conjugation efficiency of the modified DTPA-bound nanospheres determined a conjugation efficiency of 74 %. The DTPA-bound nanospheres displayed a size of 105.6 nm (Figure 4), a PdI of 0.24, and a zeta potential of -31 mV. The results indicated that the DTPA-bound nanospheres provided a slight increase in the net negative charge for the zeta potential value and a comparative increase in particle size. Accordingly, the zeta potential of the modified nanospheres provided certainty that the synthesized nanospheres were physically stable.

Rheological analysis of the thermoresponsive hydrogel

Rheology studies were performed on the prepared thermoresponsive hydrogel. Stress sweep was conducted at 0.1 Hz to determine the linear viscoelastic region. At the point where the graph plunges, is where the hydrogel breaks (Figure 5a). Yield stress (Figure 5b) is the amount of force required for the deformation of the hydrogel. Studies showed that 4.558 Pa was the yield stress required for the hydrogel to flow.

Morphological analysis of the thermoresponsive hydrogel

Scanning electron micrographs of the thermoresponsive hydrogel revealed the surface morphology and architectural integrity of the lyophilized structure as depicted in Figure 6. SEM imaging depicted a porous membranous scaffold with thin undefined smooth surfaces. The pores appear large and widespread across the surface of the scaffold, detailing the potential for the hydrogel to provide for media uptake for exposure and release of the amantadine-loaded conjugated nanospheres.

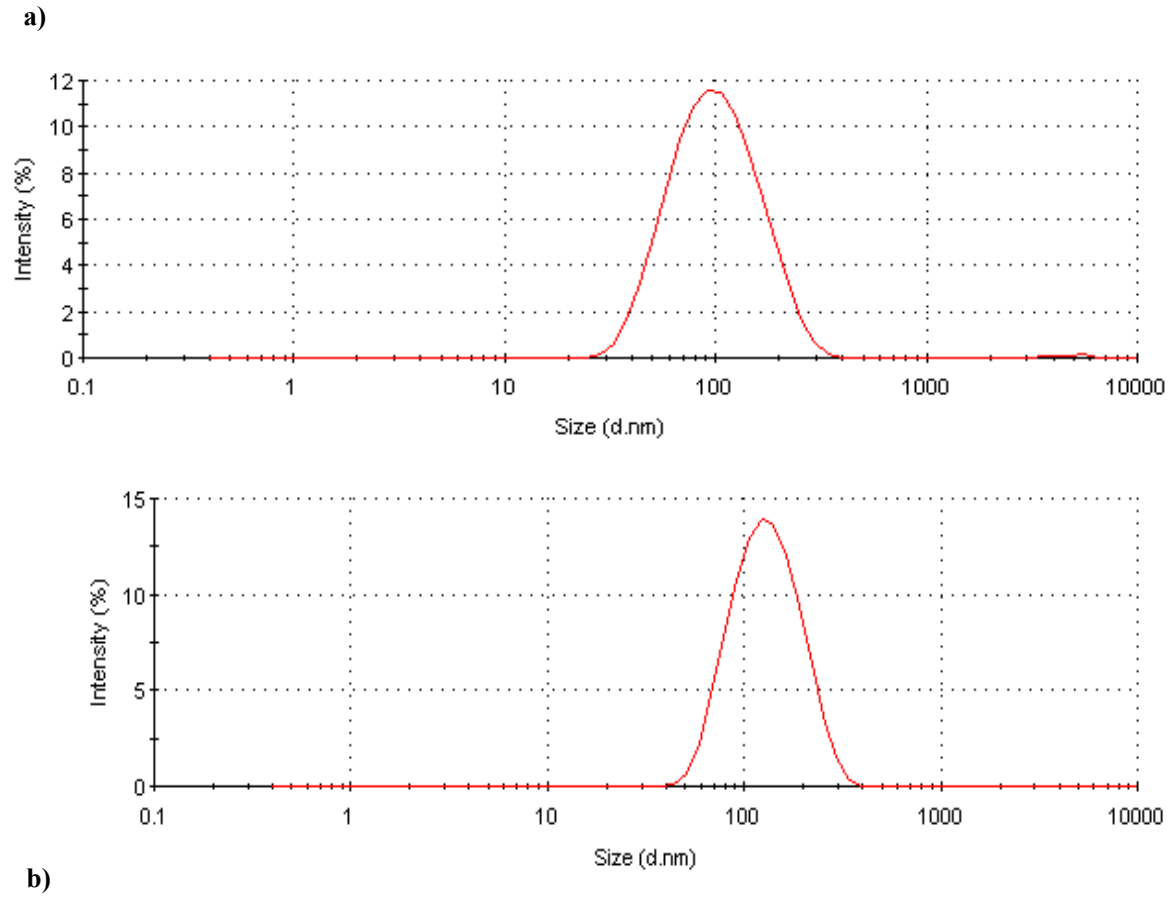

Figure 4. Comparison of the size distributions of a) the unmodified optimized nanospheres and b) the DTPA-bound optimized nanospheres.

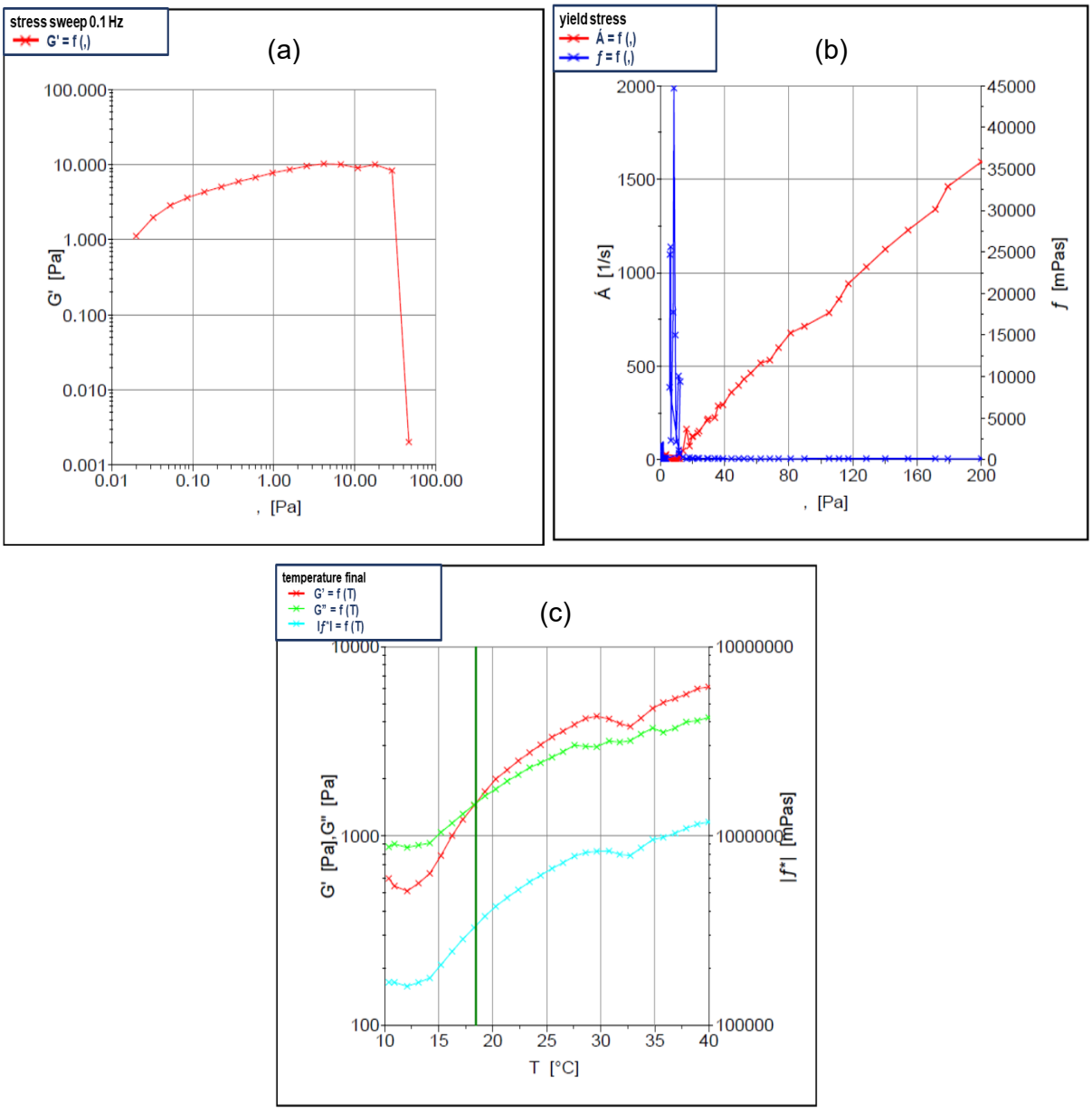

Figure 5. Rheological profiles of (a) the stress sweep of the hydrogel, (b) the yield stress of the hydrogel and (c) the temperature gelation.

In vitro amantadine release from the conjugated nanosphere-hydrogel system

The *in vitro* release profile of amantadine from the nanosphere-hydrogel composite (Figure 7) detailed that amantadine could be released from the nanosphere-hydrogel composite in a sustained manner over an extended period. Results of the nanospheres not loaded into the thermoresponsive hydrogel detailed an initial burst release (FDR of 0.43) within 3 hrs with a sustained release phase following. A FDR of 0.72 was thereafter achieved after 72 hrs detailing the potential of the prepared conjugated nanosphere system for the immediate and sustained release of amantadine. Evaluation of the conjugated nanospheres-hydrogel system detailed the sustained release of amantadine from the onset of the release study with a FDR of 0.03 achieved after 72 hrs.

Cell studies

NSC-34 cell viability was determined after exposure to different concentrations of amantadine, the drug-loaded DTPA-bound nanospheres, the drug-loaded nanospheres (without DTPA), the placebo (DTPA-bound nanospheres without drug) through an MTT assay.

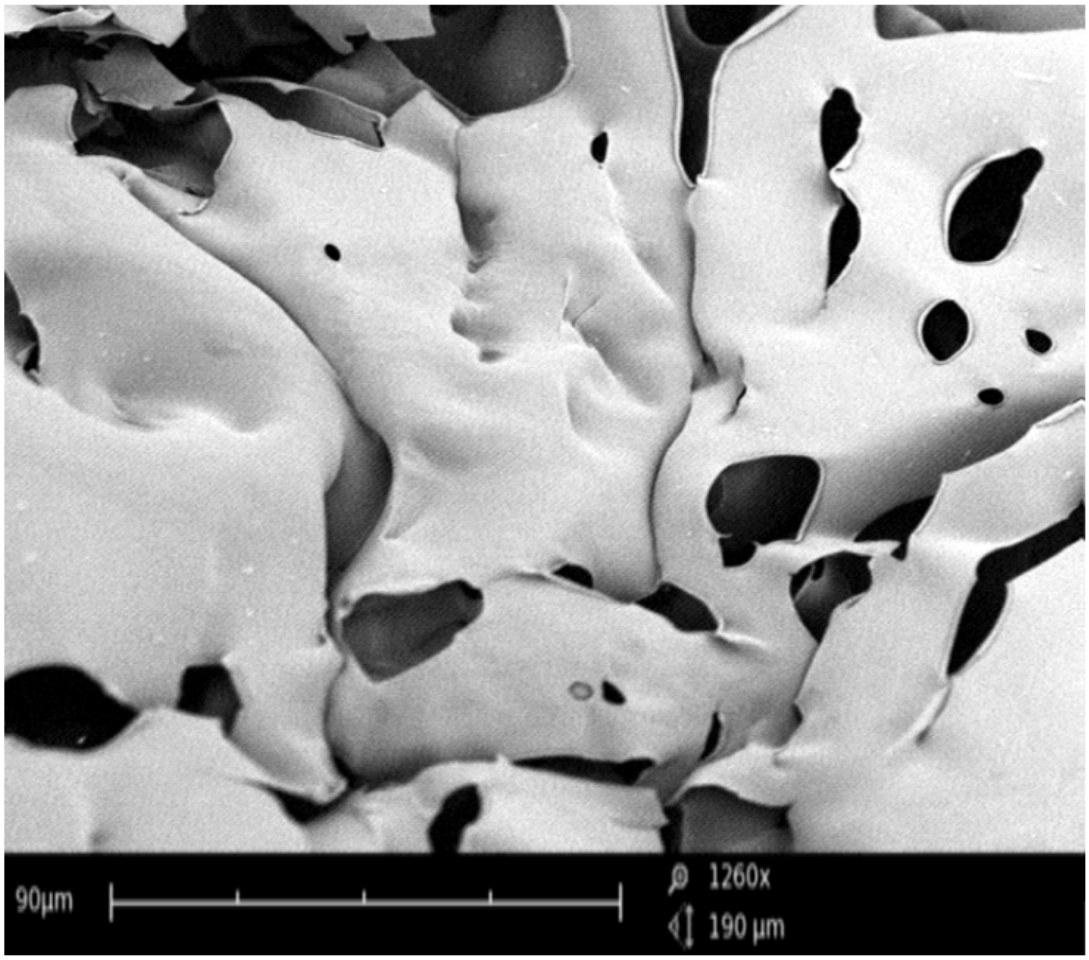

Figure 6. SEM image of the lyophilized thermoresponsive hydrogel taken at a magnification of 1260x.

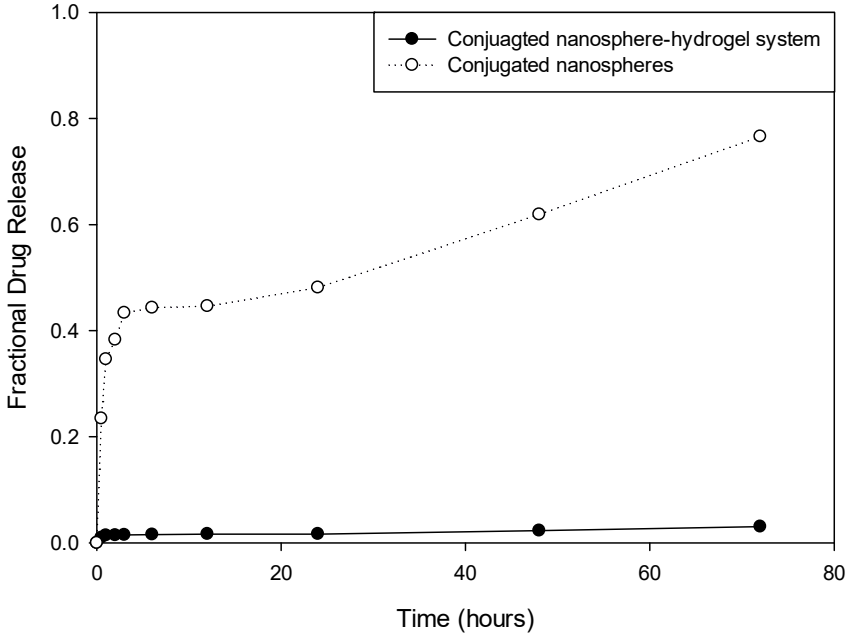

Figure 7. Comparison of amantadine released from nanospheres and nanosphere-hydrogel composite with standard deviations of $\leq 7.9481e^{-3}$ and ≤ 0.2060 respectively.

The thermoresponsive hydrogel and the nanosphere-hydrogel composite were also tested using the MTT assay at various time intervals. In the concentration-dependent cytotoxic experiment (Figure 8) the cell viability of NSC-34 decreased with an increasing concentration of the all components of the nanospheres, indicating that the cytotoxicity of the nanospheres was in a concentration-dependent manner. The results show that there was also an overall decrease in cell viability with increasing concentration confirming the results obtained. Intragroup statistical analysis (at each concentration analyzed) revealed significant variation in cell viability within each concentration interval with a $P < 8 \times 10^{-11}$ determined. Intergroup statistical analysis (analysis of a single sample over varying concentrations) revealed no significant variation between the control group (1) where 100% viability was determined at each interval. Intergroup statistical analysis of the remaining groups determined significant variation in cell viability over the concentration intervals with $P < 0.02$ in these groups.

In the time-dependent experiment to test the cytotoxicity of the nanospheres, 100 µg/mL was selected as the concentration to investigate prolonged toxicity (Figure 9). Time-dependent cytotoxicity study results show that there was a slight decrease in cell viability with increased incubation time. However, after 72 hrs the cell viability almost levels out and stops decreasing. The hydrogel and the nanosphere-hydrogel composite were also tested for prolonged toxicity (Figure 9). They expressed similar results to the nanosphere formulation in terms of time-dependent cytotoxicity. However, the hydrogel and the nanosphere-hydrogel composite showed less toxicity than the nanosphere formulation. Intragroup statistical analysis (at each time point) revealed significant variation in cell viability within each time period with a $P < 6 \times 10^{-6}$ determined. Intergroup statistical analysis (analysis of a single sample over varying time intervals) revealed no significant variation between the control group (1) where 100% viability was determined at each interval. Intergroup statistical analysis of the remaining groups determined significant variation in cell viability over the concentration intervals with $P < 0.002$ in these groups.

Ex Vivo Uptake of the Modified DTPA-Bound Nanospheres

To investigate the effect of the DTPA on nanosphere uptake, *ex vivo* samples were characterized by fluorescence imaging. Results depicted high cellular uptake of the FITC-labelled DTPA-bound nanospheres (Figure 10). Unmodified nanospheres showed no significant fluorescence activity. The DTPA-bound nanospheres had a slightly increased size as compared to the unmodified nanospheres. Small nanoparticles sediment less than larger nanoparticles and their contact with cells is determined by diffusion and convection forces. Conversely, larger nanoparticles settle more rapidly due to the additional influence of sedimentation forces. Well plates containing the DTPA-bound nanospheres were found to show slight sedimentation. It has been reported that nanoparticles with a fast sedimentation rate show higher cellular uptake (19). This study therefore demonstrated that the modified DTPA-bound nanospheres had a greater cellular uptake. This result indicated that intracellular uptake of nanospheres was mediated by the DTPA conjugated onto the nanospheres.

To supplement the uptake studies, fluorescent nanospheres were viewed under the magnification of the CellVizio® imaging system from 30 min to an hour. Figure 11 shows that DTPA-bound nanospheres were most efficiently internalized by the NSC-34 cells in comparison to the unmodified nanospheres.

DISCUSSION

The amantadine-loaded nanosphere formulations were obtained using the different preliminary variables predetermined by the 3-Factor Box-Behnken experimental design. The double emulsion evaporation technique was employed based on its advanced encapsulation of water soluble drugs in comparison to other incorporation methods (20, 21). Double emulsion solvent evaporation involved two steps where the polymer solution containing the drug was emulsified, which determined the size distribution of the nanospheres, followed by the solidifying of the nanospheres through solvent evaporation and polymer precipitation. The addition of the primary emulsion to the external aqueous phase resulted in an instant change of the solution into a turbid mixture, indicative of the spontaneous formation of nanospheres.

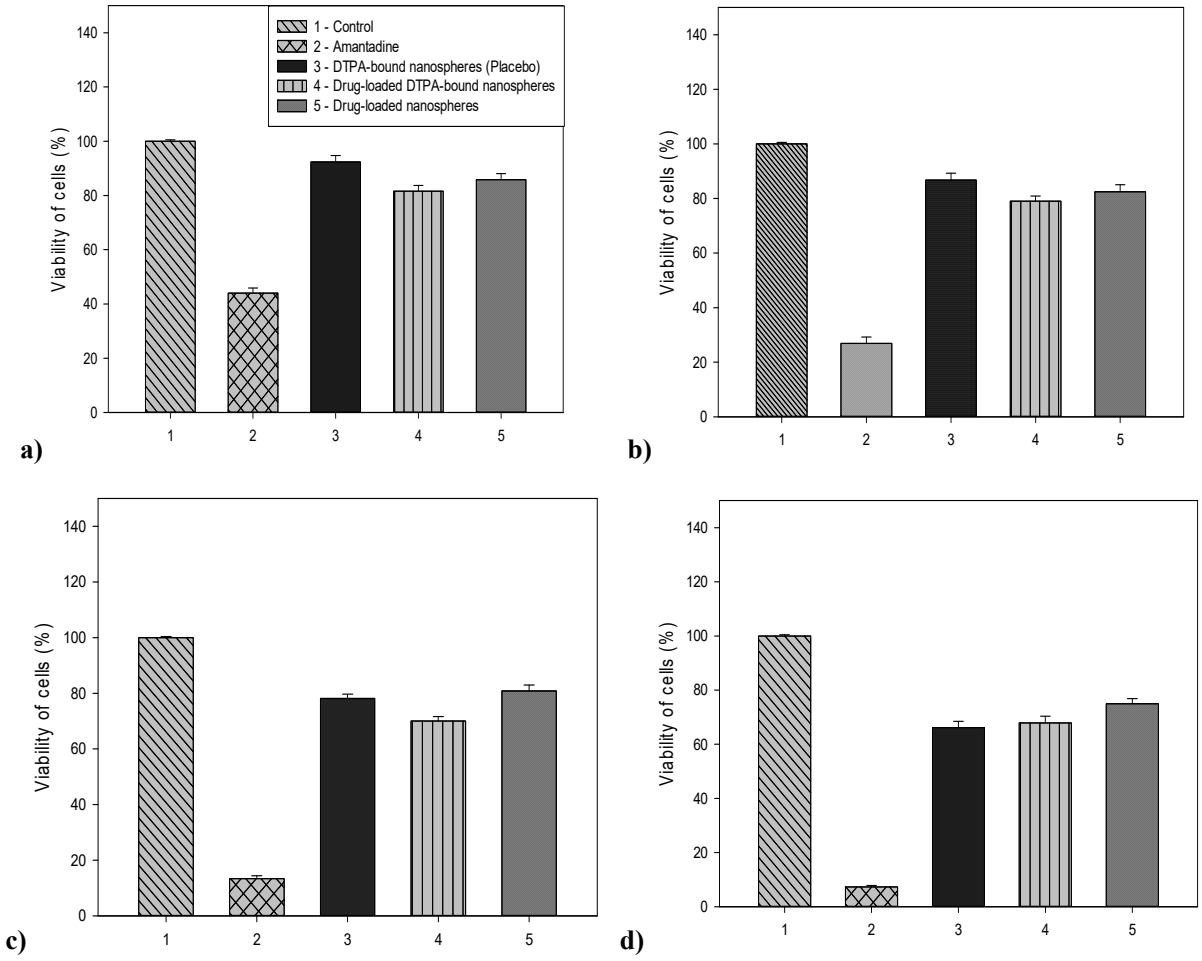

Figure 8. *In vitro* cytotoxicity of different concentrations of the various stages of the nanosphere formulation, including amantadine as the positive control and plain cells as negative control, after incubation for 48 hr; a) = 25µg/ml; b) = 50µg/ml; c) = 100µg/ml; d) = 200µg/ml, (SD ≤2.55% and $P < 0.05$ in all cases).

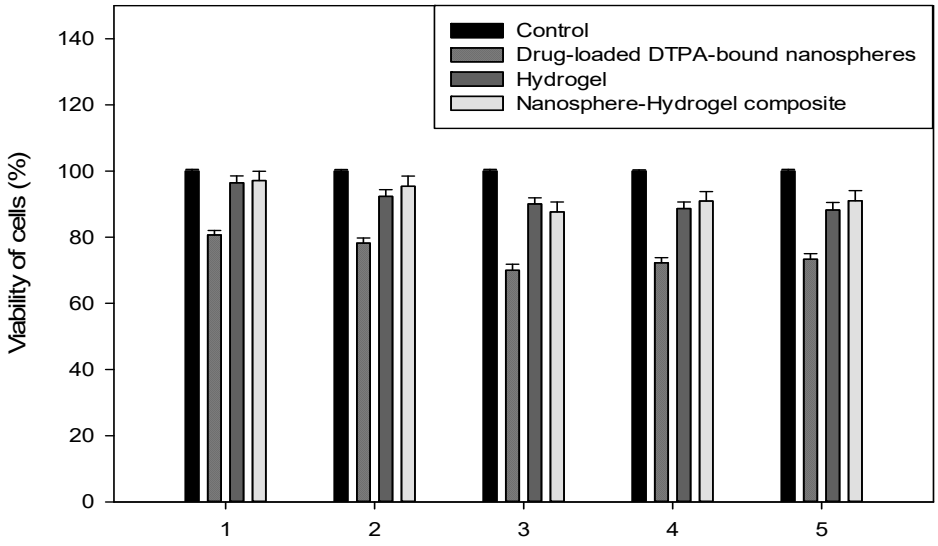

Figure 9. *In vitro* cytotoxicity of the complete nanospheres, the hydrogel and the nanosphere-hydrogel composite after incubation at different times; 1 = 12 hrs; 2 = 24 hrs; 3 = 48 hrs; 4 = 72 hrs; 5 = 96 hrs, (SD ≤3.12% in all cases).

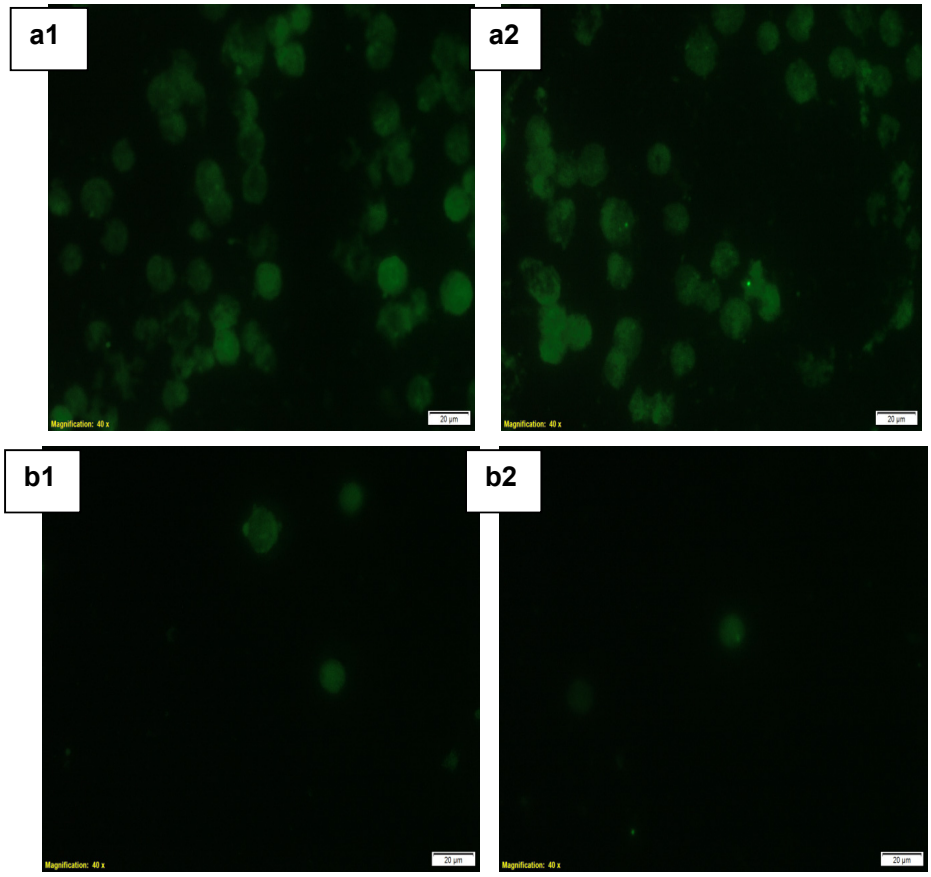

Figure 10. Fluorescent imaging of NSC-34 cell line incubated with FITC labelled a1,a2) nanospheres without fluorescence and b1,b2) DTPA-bound nanospheres.

The subsequent responses obtained for the various formulations: the nanosphere size, zeta potential, amantadine entrapment and mean dissolution time were employed for the optimization process. The results obtained from the experimental design (Table 1) were inserted into the MINITAB® software to yield ten potential optimized formulations and the selected, most suitable optimized formulation had a composite desirability (D), size desirability, zeta potential desirability and MDT desirability of 1.000. The most optimum parameters were those that displayed a desirability of 1.000 and those that had a desirability closer to 0.000 were considered the least optimum parameters. The optimal formulation had independent parameters; sonication time of 30.0 min, amount of PMA (260.0 mg) and solvent volume of 20.0 mL which produced predicted nanosphere responses of; size of 79.03 nm, zeta potential of -27.24 mV, drug entrapment of 37.28 % and a MDT of 18.27 hr.

It is well-known that nanosphere size has an effect on drug loading, drug release, and ultimately the targeted delivery of amantadine across the BBB. The prepared formulations produced nanospheres sizes between 68 and 113 nm, which is sufficient for cellular uptake as vesicles between 100-150 nm can be endocytosed at the site of action (22). The formulations displayed poly dispersity index (PdI) values of less than 0.5, which was an indication of a uniform nanosphere size distribution. The zeta potential values ranged from -14.3 mV to -29.2 mV. The increased zeta potential values indicate the high stability of the nanospheres by electrostatic repulsion forces and the net negative charge is as a result of the anionic MAC. The experimental design showed moderate entrapment efficiency of the nanospheres ranging from 19.43 to 39.75 %. A large quantity of amantadine was still in solution after phase separation.

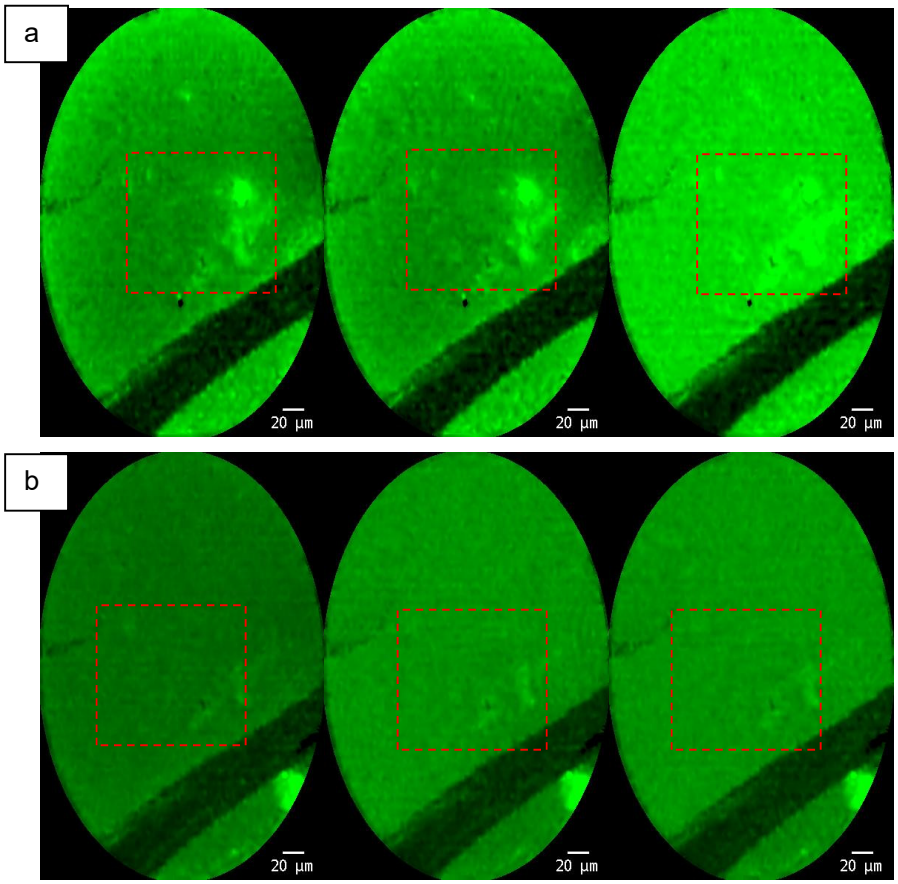

Figure 11. CellVizio® imaging of a) the DTPA-bound nanospheres and b) the unmodified nanospheres taken between 30 and 60 mins.

Evaluation of the gelation temperature displayed the characteristic pattern of a thermoresponsive system with a LCST. As illustrated in Figure 5c, the point at which the storage and loss modulus crossover (dark green vertical line) was considered the gelation temperature for the formulation. Initially, G" is larger than G', which is expected since the sample was still in liquid state, and therefore most of the energy is lost as viscous heat. As the solution starts to gel and a cross-linked network is formed, both G' and G" begin to increase; however, the rate of increase of G' is much higher than that of G" due to the elastic properties of the gelling hydrogel taking over and beginning to dominate. As a result, there is a crossover point where G' becomes larger than G". The temperature required for this crossover to occur, the gelation temperature for the solution, was therefore determined to be 18.45 °C. This result therefore determined that the prepared hydrogel would form a solid implant when exposed to physiological temperature.

The observed *in vitro* burst release of amantadine from the unconjugated nanospheres can be attributed to weak interactive forces between the amantadine and the polymers upon exposure to PBS (23). Erosion of the scaffold is due to weakening of the crosslinked bonds with exposure to PBS (pH 7.4). Hydrolysis of the ε-Caprolactone ester bonds present in the hydrogel occurs without creating a localized acidic environment upon degradation (23). Additionally, the higher copolymer concentration in the hydrogel reduced the porosity of the delivery system and imparted a greater viscosity and tortuosity (24). This result therefore determined that the prepared conjugated nanosphere-hydrogel system has the potential to act over a longer period of time for extended therapeutic effects, validating the dispersion of the nanospheres within the thermoresponsive hydrogel. In addition, DTPA is highly ionizable, therefore by incorporating the ligand into the hydrogel delivery system, environmental reactions are reduced and its

stability is enhanced allowing for a reduced drug release (25).

The undertaken cell studies determined that amantadine was more toxic in its conventional form than when encapsulated in the nano-drug delivery system, with and without DTPA, suggesting that the nanospheres were able to expose the cells to less amantadine when compared to the directly added conventional drug. In addition, the delivery system was able to release the amantadine slowly, ensuring gradual exposure of the drug to the cells. The control delivery system had no significant toxicity as VCL has been shown to support appreciable cell viability and reduced cytotoxicity due to the nitrogen atom in the caprolactam ring being directly connected to the polymer chain backbone, so should hydrolysis of the polymer occur, a toxic amide will not be a by-product (26, 27). In addition, ε-Caprolactone when polymerized, lacks bio-functional groups and has a low bioactivity, reducing its cell affinity (28, 29). Cellular imaging additionally noted appreciable uptake of the conjugated nanospheres containing amantadine. This result further validated the success of the formulated conjugated nanosphere-hydrogel system for the delivery of amantadine for the treatment of ALS.

CONCLUSION

The challenges with managing neurodegenerative disorders have brought forth the need for innovative development of drug delivery systems. This study provides for the design and development of a polymer based nano-enabled drug system for the treatment of ALS. Results of this study have determined that the prepared optimized nanosphere system successfully delivered amantadine in a sustained release manner over the drug release analysis period. Furthermore, conjugation of the optimized nanosphere system enhanced the site-specific uptake of amantadine as determined by high speed fluorescence imaging and microscopic analysis. The prepared thermoresponsive hydrogel system further provided for the sustained release of amantadine over a significantly longer period of time thereby allowing for a less required loading dose and potentially decreased side effects. Rheological analysis of the prepared hydrogel further detailed the thermoresponsive nature of the system for use under physiological temperature. The results of this study therefore provided for an innovative system for the enhanced delivery of amantadine which has the potential to provide greater therapeutic outcomes in patients suffering from motor neuron disease.

ACKNOWLEDGMENT

The financial assistance of the National Research Foundation (NRF) of South Africa towards this research is hereby acknowledged.

REFERENCES

1. Leigh PN, Ray-Chaudhuri K. Motor Neuron Disease. J Neurol Neurosurg Psychiatry, 1994; 57: 886-896.
2. Talbot K. Motor Neurone Disease. Postgrad Med J, 2002; 78: 513-519.
3. Shaw PJ. Motor Neurone Disease. BMJ, 1999; 18: 1118-1121.
4. Bedlack RS, Traynor BJ, Cudkowicz ME. Emerging disease-modifying therapies for the treatment of motor neuron disease/ amyotrophic lateral sclerosis. Expert Opin Emerging Drugs, 2007; 12 (2):229-252.
5. Bruijn LI, Houseweart MK, Kato S, Anderson KL, Anderson SD, Ohama E, Reaume AG, Scott RW, Cleveland DW. Aggregation and motor neuron toxicity of an ALS-linked SOD1 mutant independent from wild-type SOD1. Science, 1998; 281:1851-1854.
6. Barber SC, Shaw PJ. Oxidative stress in ALS: Key role in motor neuron injury and therapeutic target. Free Radic Biol Med, 2010; 48:629-641.
7. Bragagni M, Mennini N, Ghelardini C, Mura P. Development and Characterization of Niosomal Formulations of Doxorubicin Aimed at Brain Targeting. J Pharm PharmSci, 2012; 15(1): 184-196.
8. Hughes GA. Nanostructure-mediated drug delivery. Nanomedicine: Nanotechnology, Biology and Medicine, 2005; 1: 22-30.
9. Roney C, Kulkarni P, Arora V, Antich P, Bonte F, Wu A, Mallikarjuana NN, Manohar S, Liang H, Kulkarni AR, Sung H, Sairam M, Aminabhavi TM. Targeted nanoparticles for drug delivery through the blood–brain barrier for Alzheimer's disease. J Control Release, 2005; 108: 193-214.
10. Ganta S, Devalapally H, Shahiwala A, Amiji M. A review of stimuli-responsive nanocarriers for drug and gene delivery. Journal of Controlled Release 2008; 126: 187-204.
11. Caló E, Khutoryanskiy VV. Biomedical applications of hydrogels: A review of patents and commercial products. Eur Polym J, 2015; 65: 252–267.
12. Klouda L, Mikos AG. Thermoresponsive hydrogels in biomedical applications – a review. Eur J Pharm Biopharm, 2008; 68(1): 34–45. doi:10.1016/j.ejpb.2007.02.025.
13. Kontoghiorghes GJ. New Concept of Iron and Aluminium Chelation Therapy with Oral L1

(Deferiprone) and other Chelators. Analyst, 1995; 120: 845-851.
14. Darwish IA, Khedr AS, Askal HF, Mahmoud RM. Use of Oxidation Reactions for the Spectrophotometric Determination of Acyclovir and Amantadine Hydrochloride in their dosage forms. ACAIJ, 2005; 1(1-2):1-9.
15. Najafi A, Hutchison N. The use of DTPA diactivated ester in coupling DTPA to proteins. International Journal of Radiation Applications and Instrumentation. Part A. Applied Radiation and Isotopes, 1986; 37: 548-550.
16. Spanoghe M, Lanens D, Dommisse R, Van der Linden A, Alderweireldt F. Proton relaxation enhancement by means of serum albumin and poly-l-lysine labeled with DTPA-Gd3+: Relaxivities as a function of molecular weight and conjugation efficiency. Magnetic Resonance Imaging, 1992; 10: 913-917.
17. Klykov O, Weller MG. Quantification of N-hydroxysuccinimide and Nhydroxysulfosuccinimide by hydrophilic interaction chromatography (HILIC). Anal Methods, 2015; 7:6443-6448.
18. Wu Q, Wang L, Fu X, Song X, Yang Q, Zhang G. Synthesis and self-assembly of a new amphiphilic thermosensitive poly(N-vinylcaprolactam)/poly(ε-caprolactone) block copolymer. Polym Bull, 2014; 71: 1-18.
19. Lison D, Huaux F. Ups and downs of cellular uptake. Nat Nanotechnol, 2011; 6: 332-333.
20. Dhanaraju MD, Vemaa K, Jayakumar R, Vamsadhara C. Preparation and characterization of injectable microspheres of contraceptive hormones. Int J Pharm, 2003; 268: 23-29.
21. Ravi S, Peh KK, Darwis Y, Murthy BK, Singh TRR, Mallikarjun C. Development and Characterization of Polymeric Microspheres for Controlled Release Protein Loaded Drug Delivery System. Indian J Pharm Sci, 2008; 70(3): 303-309.
22. Kim HR, Gil S, Andrieux K, Nicolas V, Appel M, Chacun H, Desmaële D, Taran F, Georgin D, Couvreur P. Low-density lipoprotein receptor-mediated endocytosis of PEGylated nanoparticles in rat brain endothelial cells. Cell Mol Life Sci, 2007;64(3):356-364
23. Harilall S, Choonara YE, Modi G, Tomar LK, Tyagi C, Kumar P, du Toit LC, Iyuke SE, Danckwerts MP, Pillay V. Design and Pharmaceutical Evaluation of a Nano-Enabled Crosslinked Multipolymeric Scaffold for Prolonged Intracranial Release of Zidovudine. J Pharm Pharm Sci, 2013; 16(3): 470- 485.
24. Kalia YN, Guy RH. Modeling transdermal drug release. Adv Drug Deliv Rev, 2001;48(2-3):159-172.
25. Yang Y-T, Di Pasqua AJ, He W, Tsai T, Sueda K, Zhang Y, Jay M. Preparation of alginate beads containing a prodrug of diethylenetriaminepentaacetic acid. Carbohydr Polym, 2013; 92: 1915-1920.
26. Vihola H, Laukkanen A, Valtola L, Tenhu H, Hirvonen J. Cytotoxicity of thermosensitive polymers poly(N-isopropylacrylamide), poly(N-vinylcaprolactam) and amphiphilically modified poly(N-vinylcaprolactam). Biomaterials, 2005; 26: 3055-3064.
27. Ramos J, Imaz A, Forcada J. Temperature-sensitive nanogels: poly(N-vinylcaprolactam) versus poly(N-isopropylacrylamide), Polym Chem, 2012; 3(4):852.
28. Lee HU, Jeong YS, Jeong SY,Park SY, Bae JS , Kim HG. Role of reactive gas in atmospheric plasma for cell attachment and proliferation on biocompatible poly(ε-caprolactone) film. Appl Surf Sci, 2008; 254: 5700-5705.
29. Huot S, Rohman G, Riffault M, Pinzano A, Grossin L, Migonney V. Increasing the bioactivity of elastomeric poly(ε-caprolactone) scaffolds for use in tissue engineering. Biomed Mater Eng, 2013; 23:281-288.